Journal of
Renewable Energy Research and Applications (RERA)

Vol. 5, No. 1, 2024, 63-72 *DOI: 10.22044/rera.2023.12715.1202*

Economic Control of Solar Photo-Voltaic Generation System using Efficient Scheme of Novel One Cycle Modulator for Direct Current Supply

M. Zaid Khan* and S. Agrawal

Department of Electrical Engineering, RajasthanTechnical University, Kota, India.

Received Date 10 February 2023; Revised Date 22 April 2023; Accepted Date 10 May 2023
**Corresponding author: mzk2meet@gmail.com (M. Zaid Khan)*

Abstract

This paper considers the context of renewable energy generation for a photo-voltaic solar generating system with a non-linear load using one cycle controller with a motor across terminals. The paper finds a comparative study of the pulse width modulator with one cycle controller, which analyses both concepts using the power sim software. The main challenge is to reject power supply disturbance. The frequency switch controls the single constant cycle and regulates direct current supply but with transients. As in the case of pulse width modulation, transients appear. In comparison, the one-cycle controlling technique rejects power supply disturbance as the constant voltage maximum power point tracker returns a reference speed value with the speed sensor, so one switching cycle is combined with a dual compensator to reject power supply disturbance as photo-voltaic solar generation resolves the supply disturbance in a closed-loop scheme using one cycle modulator. Thus in the case of the pulse width modulation technique, the ideal efficiency using the pulse width modulation controller varies from 70.45% to 75%; in the case of the novel one-cycle control modulator's excellent efficiency varies from 95.17% to 99.49%. Since switching converters efficiently control the photo-voltaic energy generation system using one cycle control modulator rather than a pulse width modulator, apart from the swift transient response, one-cycle control modulator imparts economically efficient reference tracking and robustness to the system. The outcome of the one-cycle controller and pulse width modulated controller validates the analysis of variance (ANOVA).

Keywords: *Proportional Integrator (PI), DC to DC Buck and Boost, DC to DC Boost Converter, Maximum power point tracking (MPPT), Pulse Width Modulation (PWM).*

1. Introduction

Many types of research works have gone through to convert photo-voltaic energy into electricity. To improve the single-cycle control strategy of high-voltage boost multi-cell converters, the outcome with several advantages of the method, indicating its high feasibility and broad applicability. In the year 2020, To analyze the digital signal processor, the DSP-based One Cycle Control (OCC) strategy for the Power Factor Corrector (PFC) rectifier, which showed immunity to Common-mode voltage (CMV). The outcome if the PFC can reach the UPF state, and if the phase voltage is only affected by CMV, the phase current is free of CMV, as is the lead-lag-compensator LLC concerning the average phase current. [1-3]. The following year, 2021, five-level multi-level converter-based MV regenerative AC electronic load with one-cycle control (OCC) based on five-level diode-clamped multi-level converters with feedback design and any impedance load, in the same year proposed 2021, a one-cycle control (OCC) inverter study proposed.

This study proposed a sensor less grid voltage protection scheme for OCC-based single-phase inverter systems. Sensor-less control of the mains voltage has reduced costs and increased operational reliability. However, various sensors implement protection mechanisms of one-cycle control (OCC) to achieve one-cycle control by maintaining circuit power balance in each switching cycle [4-7]. In 2022, research works on custom power devices (CPDs) provided better harmonic mitigation when connected in parallel with the distribution grid [8-10]. In 2022, a study carried out to improve the performance of a new active power filter (APF) using a one-cycle control scheme is to apply a conventional one-cycle control strategy to an APF based on the unipolar operation [11]. In the same year, 2022, the research compared and analyzed the

performance of one-cycle control (OCC), hybrid one-cycle proportional-integral control (OCC-PI), and conventional PI control methods applied to non-inverting Buck-Boost converter. The hybrid OCC-PI control method combines OCC and PI control techniques to provide a hybrid closed-loop non-linear control technique for controlling buck-boost converters. The simulation results show that hybrid OCC PI control has a faster response speed and less output voltage overshoot than PI. It also provided better reference voltage tracking compared to the OCC control method [12].

Additionally, a study conducted in the same year, 2022, found that three-phase converters with power factor correction (PFC) enabled step-down, lower voltage stress on components and optimally designed next-generation DC-DC stages have been attractive for power conversion in next-generation data centers. An improved three-phase Swiss rectifier (PFC) buck converter is proposed based on the harmonic current injection (HCI) concept. The improved Swiss rectifier and closed-loop OCC principles were analyzed in detail and verified in simulations with an 80 kHz, 300 V, 2 kW digital controller prototype. At rated conditions, the input current THD was < 2% [13]. Moreover, another study from 2022 found several ways to mitigate and compensate for voltage disturbances. One way was to use a multilevel STATCOM. Multi-level inverters develop for the following advantages: 1. Appropriate output waveforms (voltage and current) widely used in various parts of power systems and industries. There had numerous controllers for multistage STATCOM control. Simple and inexpensive regulators included single-ended regulators commonly used in DC/DC and DC/AC converters. This article proposed a new structure to improve the performance of single-cycle regulators. Improvements include voltage dips and swells, voltage disturbances, harmonics, and short outages. To demonstrate the performance of the proposed controller, a multi-stage STATCOM was also tested and compared with the conventional PWM controller. The simulation results showed that the multi-level STATCOM corrects the disturbance. In 2023, a research paper investigates the evolutionary phenomenon of hybrid scale bifurcation in single-ended control (OCC) single-inductor dual-output (SIDO) bucks DC-DC converters. It derived single-cycle and cross-cycle iterative mapping models of OCC-SIDO converters in four operating modes to describe the dynamic information under different topology switching sequences. Numerical simulations identified second evolutionary trends in the branching behavior of hybrid scales. Third, a divergence analysis was performed based on the proposed model via eigenvalue trajectories. Significantly, the mechanism of occurrence of hybrid-scale divergence in evolutionary phenomena is described in detail. Participation factors were then used to analyze relationships between variables and eigenvalues. This provides much design-oriented information for avoiding branching behavior on a hybrid scale. Finally, P Spice circuit simulations and hardware experiments were performed to validate the analysis results [16, 17]. This paper uses the CV method with the perturbed and observed algorithm to track the maximum power and regulate the power supply across non-linear loads. The algorithm tracks the power delivered to the DC motor. Two power stages, one for each task, are required to demand and deliver quality DC power to power loads and track maximum power:

- The MPP algorithm for tracking to achieve optimized performance figures.
- The DC-fed buck-boost converter determines that the PV module is operating at the calculated optimum point.
- Need a DC-DC converter to boost the voltage.
- As a voltage regulator connected via the DC bus.
- The scheme is connected to a DC motor via a voltage-carrying DC bus regulation to obtain the output power.

Therefore, OCC analyzes the dynamic response and disturbance rejection to track the DC bus's maximum power and output modulation. Existing PV power generation systems are similar to DC-DC converters that generate PWM. Compared to the PWM techniques, OCC can cancel steady-state errors in transients. OCC is said to be more efficient regarding reaction speed, track referencing, interference suppression, and dynamics. OCC technology applies to power factor correction, multiple input converters, and MPPT. Therefore, after a mono-switching cycle, the transition to the mean value is reached by switching variables and maintaining equilibrium. Finally, Section 7 concludes when solar radiation intensity and PV module temperature are varied. Therefore, the MPPT algorithm with OCC reads the PV panel variables and calculates the optimal duty cycle. OCC, as a technology, is an indirect novel way of controlling the dynamics associated with the mean instantaneous value of a variable.

2. System description

As a system, a PV module with an OCC-based algorithm following MPPT. Simple PI control applies the voltage with a constant value using the MPPT method, as shown in figure 1. The voltage of the PV module (Vpv) and PV output power (Ppv) response to calculate the peak power operating on a calculated operating point of DC to DC buck to boost track all the points independently concerning radiation and temperature. As another converter is required to supply a constant DC output, it boosts with OCC voltage regulator output, as shown in figure 3(b)(c). It elevates and regulates the voltage supplied to the load. Thus the PV panel is connected to the OCC controller to the DC bus for balancing power, where:

Symbol	Meaning
C_1	Capacitance (μF)
C_2	Capacitance (μF)
C_3	Capacitance (μF)
L_1	Inductance (Henry)
L_2	Inductance (Henry)
D_{b1}	Diode for branch 1
D_{b2}	Diode for branch 2
M_{b1}	MOSFET for branch 1
M_{b2}	MOSFET for branch 2
V_{pv}	PV voltage (volts)
I_{pv}	PV current (amp.)
P_{pv}	Power PV (watt)
V_s	Source voltage (volts)
V_o	Output voltage (volts)
V_g	Gate triggering voltage (volts)

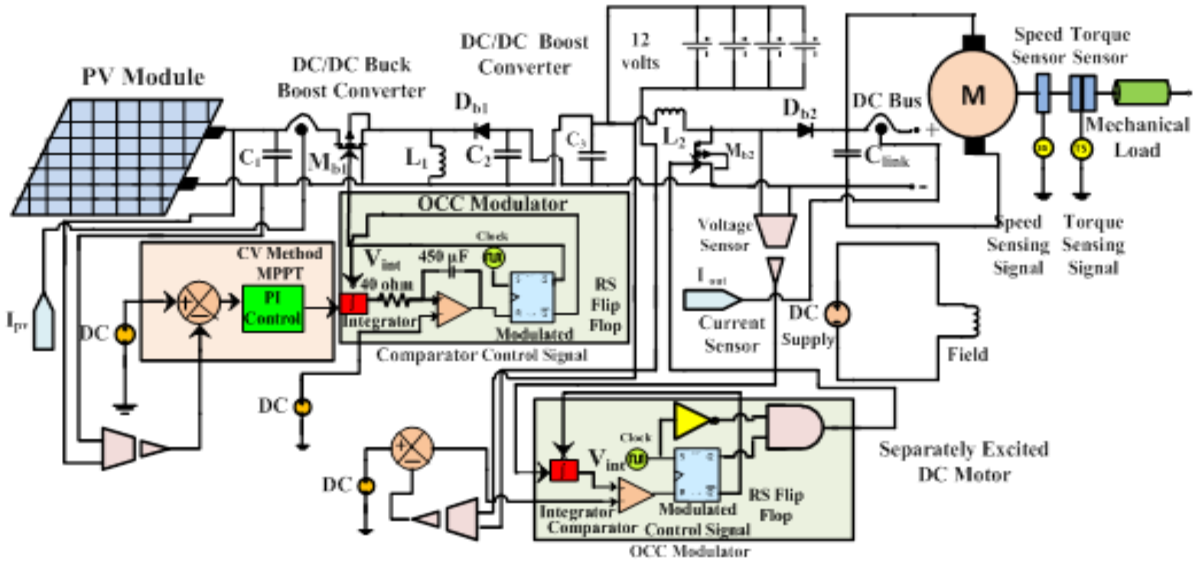

Figure 1. Modelling of PV generation system with OCC on Power Sim software.

3. One Cycle Control (OCC)

In this technique, the OCC technique controls the carrier wave amplitude as controlled in PWM. The OCC technique responds quickly to its dynamics, stabilized output, disturbance cancellation, and excellent performance. [1] The scheme of OCC resets the integrator. Moreover, a controller and comparator generate a clock signal as an RS flip-flop and a switch motion. The output means magnitude is regulated momentarily within a single switching operation, as shown in figure 2. As the switching period of the oscillator is constant. Thus as an RS flip-flop and a switch, the period is represented as t_{ON}, then the switch remains turned off as shown t_{OFF}, as the switch turns on then TS = t_{ON} + t_{OFF}, the switching variable crosses the input signal x(t) and the output signal y(t). The output signal y(t) in equation (1):

$$\mathbf{y(t) = x(t)\ ,\ 0 \le t \le t_{ON}}$$
$$\mathbf{y(t) = 0\ \ \ ,\ t_{ON} \le t \le T_s} \quad (1)$$

As the switching period, y(t) is the average value calculated by:

$$\bar{y} = \frac{1}{T_s}\int y(t)dt = \frac{1}{T_s}\int_0^{t_{ON}} x(t)dt \quad (2)$$

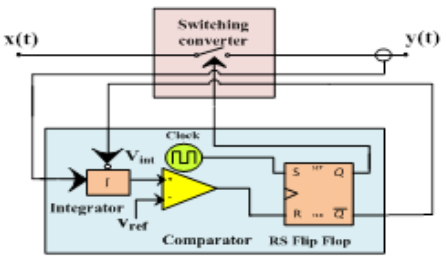

Figure 2. Basic controller for single cycle constant frequency switch.

where:

Symbol	Meaning
V_{int}	Integrator signal
y(t)	Output signal
x(t)	Input signal
t_{ON}	On time (second)
T_s	Clock duration (μs)
d(t)	Duty cycle (second)
V_{ref}	reference voltage (volts)

As the reference voltage $v_{ref}(t)$ controls the duty cycle d, it represents $d = t_{ON}/T_s$. As one cycle controls, the oscillating frequency is more significant than input x(t) and $v_{ref}(t)$. Thus the signals with a constant are associated with the clock period. Hence, $v_{ref}(t) = V_{ref}$, $x(t) = X$. Therefore, the clock sets the input connected with the RS flip-flop. Instantaneously, the clock displays one as the output as Q feeding logic level 0, so turn off the switch by which Q assumes as a logic level which resets the integrator. Therefore, the duty cycle equates the signal at output y(t) equal to the reference voltage v_{ref} (t) or

$$\frac{1}{T_s}\int_0^{t_{ON}} x(t)dt = v_{ref}(t) \quad (3)$$

As flip-flop takes logic, level 1 input resets. It makes Q level 0, which leads the integrator output to zero. The clock reaches one as the cycle repeats itself. Thus the reference voltage equates the output signal for each cycle as T_s as constant. Therefore, the modulation of the duty cycle for OCC in each switching period equates the mean output signal to the reference signal with a mean magnitude as v_{ref} (t). Hence,

$$\overline{y} = V_{ref} \quad (4)$$

Figure 3(a) shows direct current alters from 1.5 amp. to 3.75 amp. to achieve OCC waveforms. As the signal x(t) for 3 ms, the value of V_{ref} is 1 volt, and the clock frequency is 20 kHz (T_s = 50 ms). Since in every cycle, the carrier V_{int} approaches the same as the reference value V_{ref} and the RS flip-flop output Q d(t), toggle from logic level 1 to logic level 0 until another cycle begins. So it is one cycle control. For example, to calculate the average value for a cycle between 150 and 200 ms, it is obtained as 1 volt. Figure 3 (a) shows direct current alters from 1.5 amp. to 3.75 amp. to achieve OCC waveforms. As the signal x(t) for 3 ms, the value of V_{ref} is 1 volt, and the clock frequency is 20 kHz (Ts = 50 ms). Since in every cycle, the carrier V_{int} approaches the same as the reference value V_{ref} and the RS flip-flop output Q d(t), toggle from logic level 1 to logic level 0 until another cycle begins. Thus it is one cycle control. For example, to calculate the average value for a cycle between 150 and 200 ms, it is obtained as 1 volt.

3.1. OCC based on MPPT

A tracker algorithm is required to get the peak power point in the PV generation system. The PV module tracks variables in this algorithm and calculates the best operating point. It is applied to modulate the signal for boost conversion at DC—an example of a PV module characteristic curve. As the radiation on the PV module depletes, the optimum output falls, as shown in figure 3. Therefore, OCC with MPPT algorithm with DC-DC converter for better performance. It graphically uses simulation tests. In this manner, the module reaches the maximum magnitude of the PowerPoint.

3.2. Maximum power points for different solar radiation intensities

A single sensor (PV output voltage) is incorporated to reach a simple control loop of MPP. As shown in table 1, the CV as perturbed and observed method proved satisfactory in tracking maximum power points (MPP). When the irradiation is 400 W/m^2, the output power of the PV module is 22.135 watts. The value for ideal MPPT efficiency for 1000 W/m^2 and 400 W/m^2 is 99.49% and 97.81%, respectively. Even at lower radiation intensities, such as 400 W/m^2, the MPPT reaches an efficiency of 97.81% tracking maximum power points (MPP). When the irradiation is 400 W/m^2, the output power of the PV module is 22.135 watts. The value for ideal MPPT efficiency for 1000 W/m^2 and 400 W/m^2 is 99.49% and 97.81%, respectively. Even at lower radiation intensities, such as 400 W/m^2, the MPPT reaches an efficiency of 97.81 %.

Table 1. Measured power (Watt) for different solar radiation (On Power Sim software).

Solar radiation in 25 ºC (W/m^2)	Measured power tracked (W)	Maximum power (W)	Ideal MPPT efficiency using PWM%
1000	42.310	31.73	74.99
800	32.730	24.544	74.98
600	19.245	14.421	74.92
400	12.750	9.361	73.41
200	9.450	6.657	70.45

3.3. Voltage regulation-based OCC

Since PV modules configure the boost converter at DC with OCC, the frequency clock with a constant pulse simultaneously turns on the MOSFET as MOSFET is an activation element after initiating its switching period. Since PV modules, the integrator configures the boost

converter at DC with OCC. Thus the frequency clock with a constant. Thus the conduction of current for the MOSFET stopped; hence, diode is switched on. The switching voltage diode is the difference between the input and output voltage across the output v_{out}. The voltage across the diode vs is:

$$V_s = \frac{1}{T_s}\int_0^{DT_s} (v_s - v_{out})dt \quad (5)$$

As the voltage across the diode is Vs, since the difference between diode voltage vs and output voltage vout. Therefore, the OCC equates the integrator input, and the integrator resets and sets after receiving a signal from the flip-flop. Thus the duty cycle of the mean magnitude of the variable for switching accomplishes within one switching cycle for overcoming the transient condition. Hence, single-cycle control rejects disturbances and nullifies PWM control's demerits. Thus this method is a constant voltage (CV) algorithm of MPPT—the simulation outcomes, as shown in figure 4.

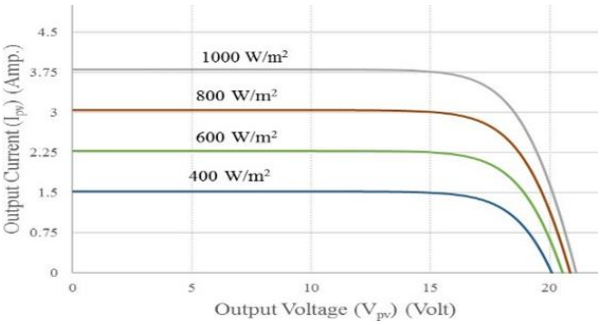

Figure 3(a). I-V characteristics obtained from PV Solar Module (On Power Sim software).

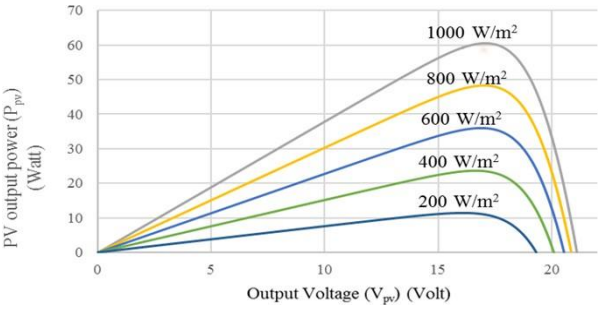

Figure 3(b). P-V characteristics curve traced STC at T = 38 ºC (On Power Sim software).

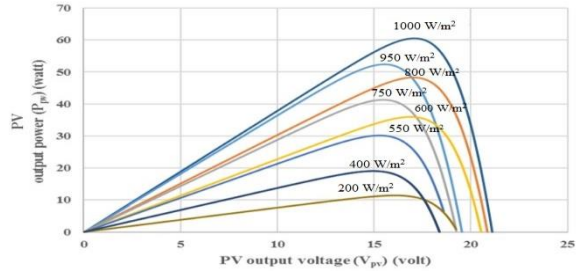

Figure 3(c). P-V characteristics curve traced STC at T = 38 ºC with intermediate irradiances (On Power Sim software).

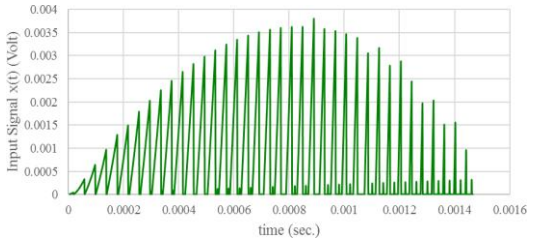

Figure 4(a). Input signal x(t) (volts) fed to MOSFET.

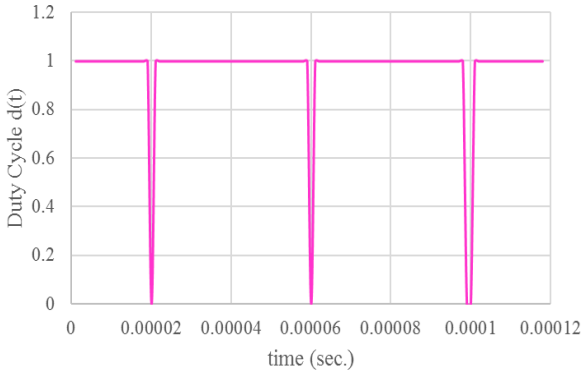

Figure 4(b). Duty cycle d(t) taken after pulse generation at gate terminals.

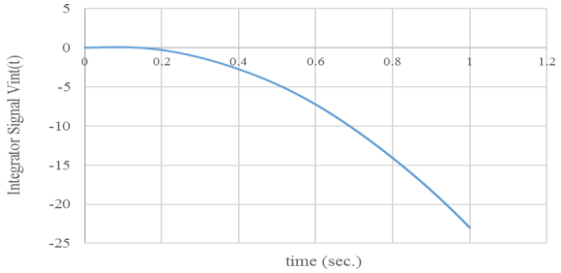

Figure 4(c). Integrator signal $V_{int}(t)$ of MOSFET.

Table 2. Measured power (Watt) for different solar radiation (On Power Sim software).

Solar radiation in 25 ºC (W/m²)	Measured power tracked (W)	Maximum power (W)	Ideal MPPT efficiency using PWM%
1000	42.310	31.73	74.99
800	32.730	24.544	74.98
600	19.245	14.421	74.92
400	12.750	9.361	73.41
200	9.450	6.657	70.45

4. Output of simulation

The PV system of the simulation in figure 4 is simulated in Power Sim to improve the tracker algorithm. It regulates the controller to optimize its performance. Thus solar and load variations perturbations are analyzed to achieve the system's dynamics. Hence, it is necessary to compare PWM and OCC to verify MPPT performance and DC bus voltage (V_{out}). The dynamics are analyzed to improve the regulation of the controller. The two resistors connected to the DC bus for switching.

4.1. MPPT algorithm analysis

The objective is to show the performance of PWM and OCC-based algorithms based on the MPPT.

The PSIM platform simulates PWM control and OCC methods separately on the same PV system. It calculates the best operative point related to the maximum power voltage at the PV module (17.3 volts). Hence, it generates a modulated control signal based on calculation. PI control parameters are tuned and prove the application and performance parameters of the proposed technique in PV systems. Thus the gain and time constant are 0.000000022 and 0.0000000000125. Moreover, the MPP tracker with an OCC modulator consists of an integrator. The controller resets and functions like a comparator that compares the resettable integrator output with a reference. Since RS flip-flops to toggle, its output per the clock signal frequency is 50 kHz. Hence, the resettable integrator input tends to be zero. Therefore, the CV MPPT algorithm minimizes the difference in reading PV voltage and reference of maximum power and voltage. In the first simulation, the energy radiation is varied by connecting 100-ohm resistance. The irradiation value is between 400 W/m^2 to 1000 W/m^2 since the MPPT tracks the output power at 17.3 volts of voltage at MPP, independent of solar radiation intensity. In the PWM-based method, undesirable transition ranges from 400 W/m^2 to 1000 W/m^2. Thus the PV output voltage and the PV output power change. Thus in both PWM and OCC, the irradiance is 1000 W/m^2, and the output power of the PV module is 60.534 watts. When the PWM has implemented solar radiation drops or increases from 400 W/m^2 to 1000 W/m^2, the voltage of PV reaches its steady state conditions after a transient. Whereas in the case of OCC, the voltage reaches its stationary conditions without transient. Thus the diversion of PV voltage of 5 volts from its reference. As a result, the power loss represents rapid changes in solar radiation. Thus OCC rectifies the PI controller error. As the OCC reaches the reference value, the integrator resets, and the MOSFET stops conducting until another clock signal begins; solar radiation increases from 400 W/m^2 to 1000 W/m^2. In addition, OCC controls a triangular carrier wave to generate a larger pulse to switch the MOSFET. Thus the higher the solar radiation, the more carrier, and the modulated signal width are more at lower intensities. Therefore, the higher the pulse width, the higher the output power of the PV module, so the higher the output current of PV.

5. Analysis of controller

When there is an alteration in the irradiation, variation in output voltage occurs. The PV voltage response where its stationary conditions without transient. The PV voltage response when the solar radiation swiftly changes from 400 W/m^2 to 1000 W/m^2, as shown in figure 5. As shown in figure 5(a), as the radiation of solar falls, the PV module output power and buck to boost converter at DC radiation falls. it works as a voltage controller. It modulates after DC-DC boost conversion, as shown in figure 5(b). The DC bus varies from 100 to 250 ohms to reach a steady state, and the voltage diversion is almost 2.5 volts from a specific time during the transient. As the load variation time and the transient last 0.008 sec, the overshoot is almost 1 volt. As OCC, that DC bus voltage does not have transients due to variations in solar radiation, as shown in figure 6(a), while in the case of PWM, DC bus voltage has transient as the solar radiation varies at 0.065 seconds by observation. Since the system is susceptible to disturbances, OCC can protect the DC bus with the loads connected to it. In PWM, DC bus voltage has transient as the solar radiation varies from 100 ohms to 250 ohms at 0.065 seconds, as shown in figure 6(b). Therefore, the method is possible to implement. Thus OCC is configured at the DC bus maintaining constant 98 volts. Therefore, OCC is applicable for multi-objective DC supply for power quality intensification. Therefore, the voltage at terminals remains stable, as shown in figure 6(c). An increase in solar radiation caused transients, which takes 0.1 second to reach a steady state, and the voltage diversion is almost 2.5 volts from a reference at a specific time during the transient. As the load variation time approaches, the transient reaches 0.008 second, and the overshoot is almost 1 volt. These techniques are for both methods for proper nullification of transients. As in the case of PWM, the switching variable is uncontrolled, so the condition of abnormal outcome arises. In the case of OCC controls, the switching variable as the abnormal response does not appear as the switching variable. OCC is more accurate as compared to PWM. So, as the abnormal condition occurs bus is regulated, which makes the system robust. Hence, results as shown on the Power SIM software.

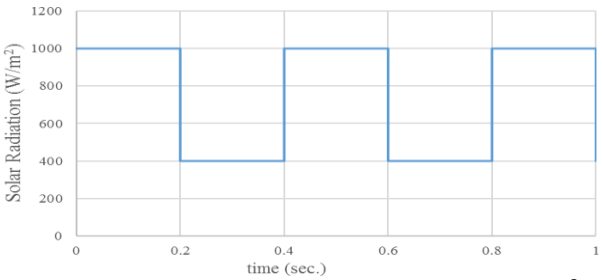

Figure 5(a). Solar irradiance variation in intensities (W/m^2).

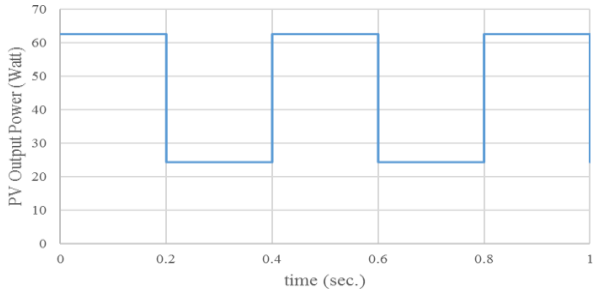

Figure 5(b). PV Output Power extracted using OCC (watt).

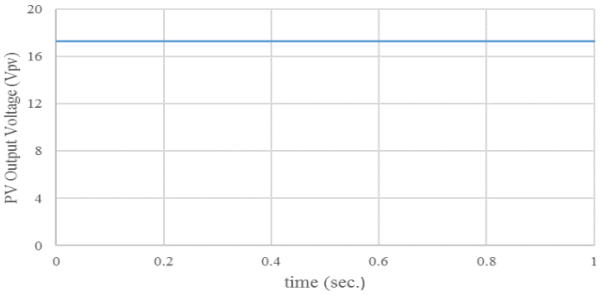

Figure 5(c). PV module at terminals of voltage sensors.

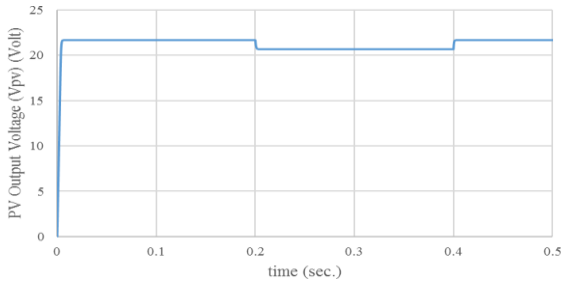

Figure 6(a). PV module voltage at terminals.

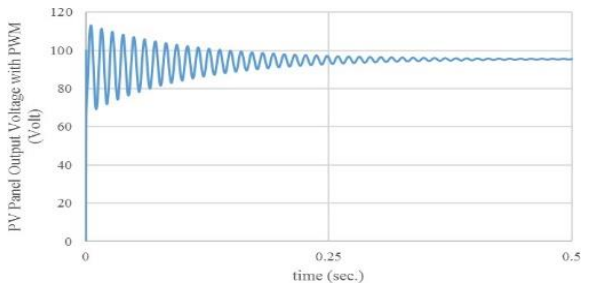

Figure 6(b). PV panel output voltage using PWM technique.

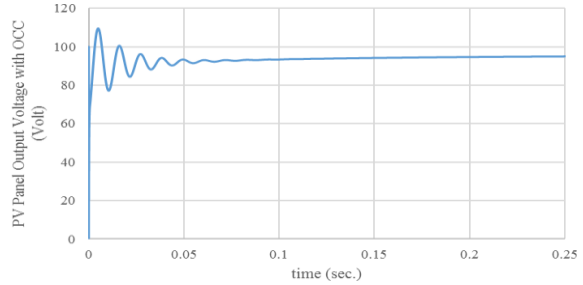

Figure 6(c). PV panel output voltage using OCC technique.

6. Results and discussion

As per the findings of solar irradiance from 400 W/m^2 to 1000 W/m^2, the duty cycle, a modulated signal of the PV solar generation system with OCC is 95.23%, and MPPT reaches efficiency from 97.81% to 99.49%, respectively. The terminal PV module voltage is 17.5 volts. The change in solar power generation from 400 W/m^2 to 1000 W/m^2 from 25 watt to 65 watt is 40 watt, as shown in figure 5(b). The output voltage with PWM is 98 volts, as shown in table 3, 4, and 5.

Table 3. Comparison of efficiencies of PWM and OCC modulator.

Solar irradiance (Watt/m^2)	PV module voltage (Volt)	Efficiency of PWM (%)	Efficiency of OCC (%)
200	17.5 V	70.45%	95.17%
1000		74.99%	99.49%

Table 4. Change in power using PWM at different solar radiation.

Solar Irradiance (Watt/m2)	PV Module Output Voltage (Volt)	Power using PWM (Watt)	Change in Power using PWM (Watt)
200	98 V	25	40 Watt
1000		65	

Table 5. Change in power using OCC at different solar radiation.

Solar Irradiance (Watt/m2)	PV Module Output Voltage (Volt)	Power using PWM (Watt)	Change in Power using PWM (Watt)
200	98 V	25	40 Watt
1000		65	

The output voltage with PWM is 98 volts maintained within the 2 volts drop as the triangular carrier wave is achieved from 60 microseconds to 148 µs in geometric progression from 1 mV to 8 mV signal, as shown in figure 7(a). Later on, 3 mV maintains from 275 ms to 300 ms. The controller with PWM with PV generation system with the duty cycle modulated signal of the PV solar generation system with PWM is 60%, as shown in figure 7(d). Thus the OCC control technique nullifies switching loss compared to the PWM technique. Thus OCC stabilizes transients compared to the PWM controller, as shown in figure 6(c). The maximum and measured power tracked using the PWM controller and OCC modulator is plotted with the intensity of solar radiation, as shown in figure 8(a)(b). The inference shows the higher maximum and measured power tracking compared to the PWM controller with the OCC controller. Similarly, the comparative measurement of power tracked for the OCC modulator shows 95.17% to 99.49% efficiency, whereas the efficiency of the PWM controller lies from 70.45% to 74.99%, as shown in table 3, also shown in figure 8(c). Similarly, at different solar radiation using PWM and OCC change in power is 40 watts, as shown in tables 4 and 5.

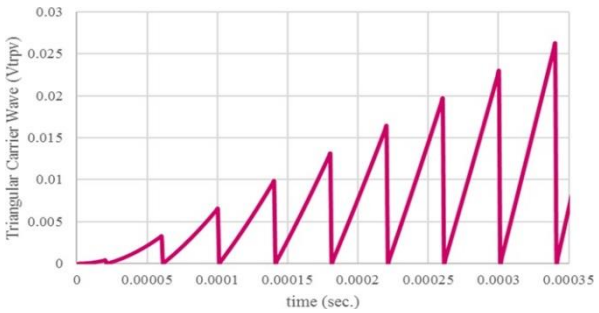

Figure 7(a). Triangular carrier wave formation after signal integration technique.

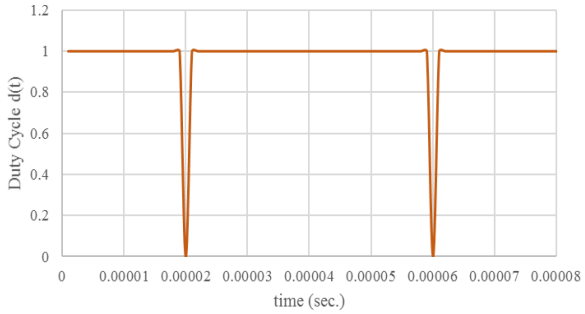

Figure 7(b). Duty cycle d(t) using OCC technique.

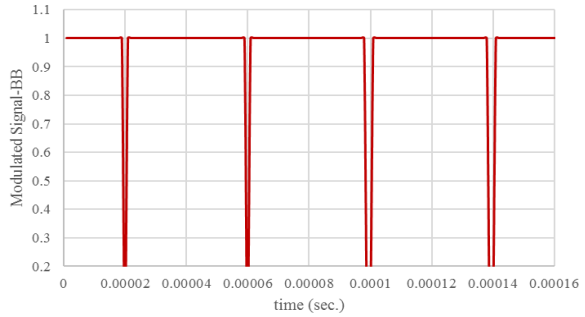

Figure 7(c). Modulated signal-BB by OCC with time (sec).

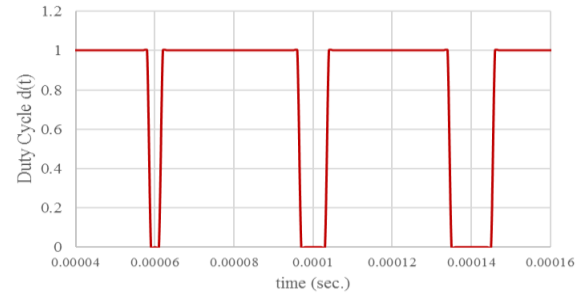

Figure 7(d). Duty cycle d(t) using PWM controlling.

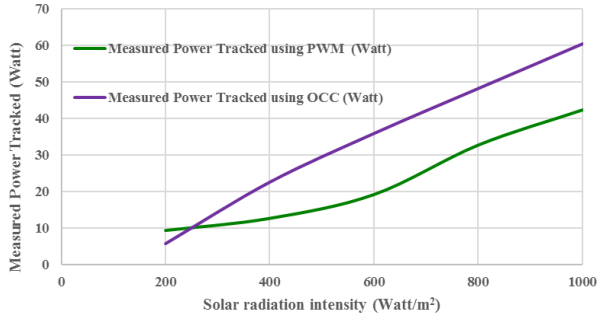

Figure 8(a). Comparative measurement of measured power tracked in (watt).

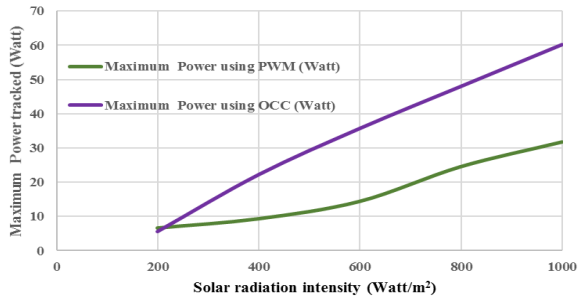

Figure 8(b). Comparative measurement of maximum power tracked in (watt).

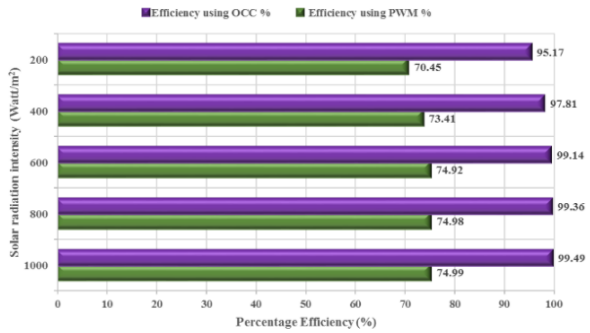

Figure 8(c). Comparative analysis of PWM controller and OCC modulator efficiencies in percentage (%).

7. Conclusion

The power loss in the system as the PV panel affects by rapid changes in solar radiation, which may damage the load connected to it. Therefore, the OCC technique has the advantage of nullifying transients for the disturbances like solar radiation. The merit is that the absence of transient can extend the life, which prevents the loads from damage. Hence, it is a multi-objective controller. The future scope of one cycle controller is with active power filters, multi-level inverters for renewable energy generation applications instead of PWM controllers in reduction of switching loss to improve the quality of power. Resultantly, while considering near regression for defining the objective function of both the OCC modulator and PWM controller, regression statistics show that the value of R-square in the case of the PWM controller and OCC modulator are 0.8443 and 0.8682, respectively, as shown in figure 9(a). Similarly, the standard error is 1.0253 and 0.8562 in the PWM controller and OCC modulator, respectively, as per figure 9(a). Since output validation using the Analysis of Variance (ANOVA) method is a proper and reliable tool, the value of F is 10.845 and 13.17 in the case of PWM and OCC, respectively. Similarly, the significance value of F is 0.0811 and 0.0682 in the case of PWM and OCC, respectively. To optimize the outcome from the controller, as mentioned above, the coefficient and intercept as per the

objective function in the case of PWM and OCC are 69.665, 0.00755, and 94.395, 0.00695, respectively, as shown in figure 9(a). The P-value of the PWM and OCC modulator is 0.0811 and 0.0682, respectively, as shown in figure 9(c) and figure 10 (a)(b). Therefore, the predicted value of the efficiency of the OCC modulator under linear regression is more significant than 94.402%, depending on the intensity of radiation, whereas, in the case of the PWM controller predicted value of efficiency is 69.672%. Therefore, based on regression statistics, the OCC modulator validates its efficient and economic control with reliability, versatility, novelty, and multi-objective application for optimization of solar power generating system performance, as shown in figure 10 (c).

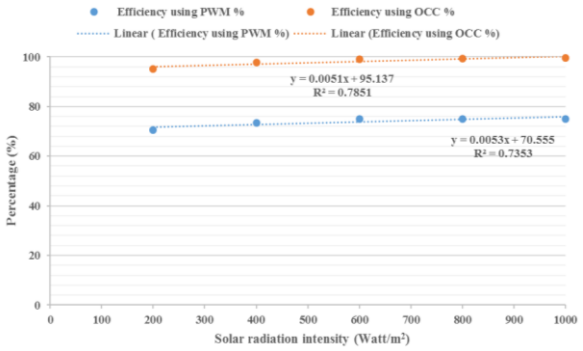

Figure 9 (a). Multiple linear regression curves for PWM and OCC modulator.

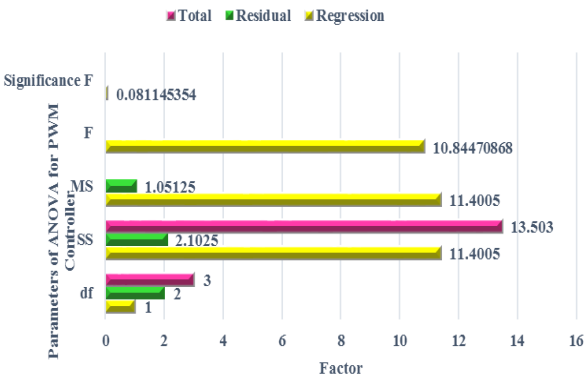

Figure 9 (b). ANOVA validation for PWM controller.

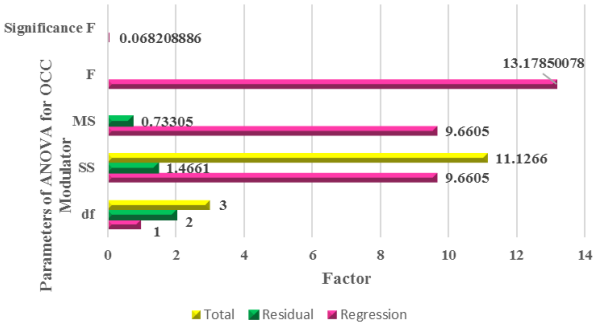

Figure 9 (c). ANOVA validation for OCC modulator.

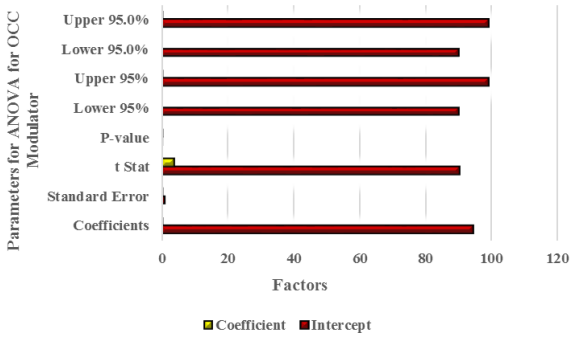

Figure 10 (a). Regression parameters for ANOVA for PWM controller.

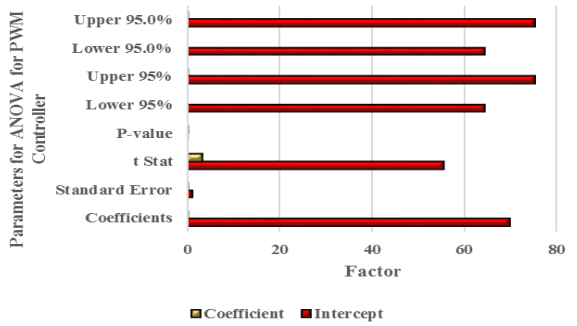

Figure 10 (b). Regression parameters for OCC modulator for ANOVA validation.

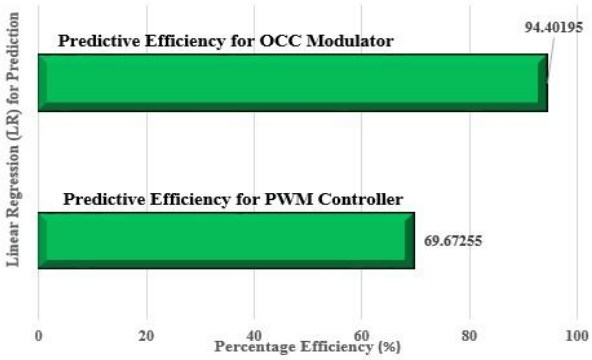

Figure 10 (c). Prediction of controller's efficiency

8. Nomenclature

OCC	One Cycle Controller
MPPT	Maximum Power Point Tracker
STATCOM	Static Compensator
PWM	Pulse Width Modulator
PSIM	Power Simulator
PV	Photo Voltaic

9. References

[1] G. Zhang et al., "Enhanced One-Cycle Control for Multicell Power Converters," in IEEE Transactions on Power Electronics, Vol. 35, No. 8, pp. 8846-8856, Aug. 2020, DOI: 10.1109/TPEL.2020.2967630.

[2] Salazar, Andres, Rodrigo Teixeira, Werbert da Silva, Guilherme Pillon, João Carvalho Neto, Elmer Villarreal, and Alberto Lock. "One Cycle Control of A PWM Rectifier a new approach."(2020). DOI:10.20944/preprints202009.0036.v1.

[3] Aboutaleb, Abdellatif M., Haitham Z. Azazi, Dina SM Osheba, and Awad E. El-Sabbe. "A four-switch shunt active filter based on one cycle control for compensating non-linear loads." International Journal of Electronics 107, no. 7 (2020): 1063-1082. DOI: https://doi.org/10.1080/00207217.2019.1692374.

[4] Jeong, In Wha. "DC-Link Capacitor Voltage Balancing Control of a Five-Level Regenerative AC Electronic Load using One-Cycle Control." Energies 14, No. 19 (2021): 6101,
DOI: https://doi.org/10.3390/en14196101.

[5] Reddy, Venkata R., and E. S. Sreeraj. "Grid Voltage Sensor-less Protection Scheme for One Cycle-Controlled Single-phase Photovoltaic Inverter Systems." CSEE Journal of Power and Energy Systems 8, No. 6 (2021): 17201729,
DOI: 10.17775/CSEEJPES.2020.04400.

[6] Y. L. Guo, L. Wang, and Q. H. Wu, "Bifurcation Control Method for Buck-Boost Converters Based on Energy Balance Principle," in IEEE Journal of Emerging and Selected Topics in Power Electronics, Vol. 9, No. 6, pp. 6947-6954, Dec. 2021,
DOI: 10.1109/JESTPE.2021.3067357.

[7] Reddy, Venkata R., and E. S. Sreeraj. "A hybrid islanding detection method for one cycle controlled PV inverter system." IEEE Journal of Emerging and Selected Topics in Industrial Electronics 3, No. 3 (2021): 777-787,
DOI: 10.1109/JESTIE.2021.3099395.

[8] Manoj, Vasupalli, Dr Prabodh Khampariya, and Dr Ramana Pilla. "Performance Evaluation of Fuzzy One Cycle Control-based Custom Power Device for Harmonic Mitigation." IJEER 10, No. 3 (2022): 765-771,
link: https://ijeer.forexjournal.co.in/papers-pdf/ijeer-100358.pdf.

[9] Hema Rani, P., K. Manikanta, Saly George, and S. Ashok. "Power Management Using One Cycle Control Strategy for Triple Input Single Output Fly Back DC–DC Converter." Electric Power Components and Systems 50, no. 11-12 (2022): 600-614,
DOI: https://doi.org/10.1080/15325008.2022.2138639.

[10] Rani, P. Hema, Arun Kumar Behera, Shyam S. Sundar, Saly George, and S. Ashok. "One cycle controlled three input three output DC to DC converter." Journal of Power Electronics 22 (2022): 94-104.
DOI: 10.1007/s43236-021-00335-4.

[11] Shao, Yiyuan, and Xueqin Wu. "One-Cycle Control Strategy for Active Power Filter Based on Current Feedback." In International Conference on Cognitive based Information Processing and Applications (CIPA 2021) Volume 2, pp. 463-473. Springer Singapore, 2022,
DOI: https://doi.org/10.1007/978-981-16-5854-9_58.

[12] Karaarslan, Ahmet, and Ali Shaibu. "Performance Analysis and Comparison of Non-Inverting Buck-Boost Converter Using PI, OCC, and Hybrid OCC-PI Control." Journal of Electrical Technology UMY 6, No. 2 (2022): 57 66.
DOI: https://doi.org/10.18196/jet.v6i2.15756.

[13] Q. Zhang, Z. Dong, D. Zhang, H. Zeng, X. Zheng, and W. Lin, "An Improved Swiss Rectifier and Its Nonlinear Control for Lower THD," in CPSS Transactions on Power Electronics and Applications, Vol. 7, No. 3, pp. 319-327, September 2022,
DOI: 10.24295/CPSSTPEA.2022.00029.

[14] Q. Zhang, Z. Dong, D. Zhang, H. Zeng, X. Zheng and W. Lin, "An Improved Swiss Rectifier and Its Nonlinear Control for Lower THD," in CPSS Transactions on Power Electronics and Applications, Vol. 7, No. 3, pp. 319-327, September 2022,
DOI: 10.24295/CPSSTPEA.2022.00029.

[15] Qiu, Yanhui and Daolian Chen. "Three-mode one-cycle controlled current-source single-stage multi-input high-frequency-link inverter." Journal of Power Electronics (2022): 1-12.
DOI: https://doi.org/10.1007/s43236-022-00517-8.

[16] Song, Jiuxu, Zhiwei Chang, Hongxia Liu, and Shuai Ding. "One-cycle controllability of high step-up Boost converter with coupled inductor." International Journal of Circuit Theory and Applications (2023),
DOI: https://doi.org/10.1002/cta.3532.

[17] Liu, Wei, Hao Zhang, Xinfeng Zhang, and Wei Liu. "Dynamical Analysis of Hybrid-Scale Bifurcation in One-Cycle Controlled Single Inductor Dual-Output Buck DC–DC Converters." International Journal of Bifurcation and Chaos 33, No. 01 (2023): 2350004,
DOI: https://doi.org/10.1142/S0218127423500049.